JOURNAL OF AIRCRAFT
Vol. 31, No. 5, Sept.-Oct. 1994

Two-Variable Method for Blockage Wall Interference in a Circular Tunnel

X. Qian* and C. F. Lo†
University of Tennessee Space Institute, Tullahoma, Tennessee 37388

A two-variable method for the blockage interference assessment in a circular tunnel has been developed. The Prandtl-Glauert equation is applied to describe the subsonic flowfield. Analytical solutions are obtained using Fourier transform technique, by either assuming a given body of revolution profile or representing the body of revolution by a source-sink distribution. Numerical examples computed by a small perturbation inviscid code TSFOIL and a panel method code PMARC are utilized to validate the developed two-variable method for open jet and closed circular tunnels. Good agreement has been found on interference pressure coefficient assessment between the solutions of the two-variable method and inviscid code predictions. Results have demonstrated that the two-variable method for circular tunnel blockage wall interference is ready for experimental verification.

Nomenclature

C_p	=	pressure coefficient
F	=	hypergeometric function
I_0, I_1	=	modified Bessel functions of the first kind
i	=	imaginary number, $\sqrt{-1}$
K_0, K_1	=	modified Bessel functions of the second kind
l	=	body length
M_∞	=	freestream Mach number
p	=	Fourier transform parameter
R	=	radius of the circular wind tunnel
S'	=	slope of a body revolution profile
U, u	=	axial velocity
V, v	=	radial velocity
x, r, θ	=	cylindrical coordinates in axial, radial, and angular directions
β	=	compressibility factor, $\sqrt{1 - M_\infty^2}$
ϕ	=	potential function
σ	=	distribution of source strength
ε	=	ratio of maximum body thickness to body length
$\overline{(\ )}$	=	quantity in Fourier transformed plane
$\vert\ \vert$	=	absolute value

Subscripts

i	=	wind-tunnel wall interference
T	=	wind-tunnel conditions
∞	=	freestream conditions

Introduction

THE new wall interference assessment/correction method requires in situ measurements of flow variables near the tunnel boundary, which is in contrast to the classic prediction method. The approaches can be classified[1] as one- and two-variable methods based upon the number of flow variables required at an interface near the tunnel wall. The one-variable method uses one measured variable and the representation of the test model to calculate the wall interference. The two-variable method uses two measurements at the test section boundary, but does not require any model representation. The distinct advantage of the two-variable method, in general, is able to replace the representation of a complex flowfield around the test model by the task of measurement of two flow variables.

The two-variable method applied to a two-dimensional wind-tunnel case has been reported by Lo[2] with some analytical examples. This article presents the formulation and results of the two-variable method for the blockage interference in a circular tunnel as the continuation effort. The Prandtl-Glauert equation is chosen to describe the flowfield in the subsonic flow regime. The Fourier transform technique is utilized to obtain the analytical solution. The numerical examples computed by a small perturbation inviscid code[3] and a panel method code PMARC[4] are used to validate the present results for both open jet and closed tunnels.

Formulation

A body of revolution model located at the centerline of a circular wind tunnel forms an axisymmetric flowfield. The Fourier transform technique is applied to the subsonic flow case to obtain the flow variables under free-air, wind-tunnel (i.e., wall interference) conditions. As shown in Fig. 1, the boundary value problem is formulated to simulate a wind-tunnel experiment including measured boundary flow variables at a selected control surface near the tunnel wall, $r = R$. The velocity components $U_T(x, R)$ and $V_T(x, R)$ are along axial and radial directions, respectively.

Solutions in Fourier Transformed Plane

The axisymmetric small perturbation equation for subsonic flows in cylindrical coordinates (x, r, θ) can be written independent of θ as

$$(1 - M_\infty^2)\frac{\partial^2\phi}{\partial x^2} + \frac{\partial^2\phi}{\partial r^2} + \frac{1}{r}\frac{\partial\phi}{\partial r} = 0 \tag{1}$$

Let $\bar{\phi}(p, \bar{r})$ be the Fourier transform of the potential function $\phi(x, r)$

$$\bar{\phi}(p, \bar{r}) = \frac{1}{\sqrt{2\pi}}\int_{-\infty}^{+\infty}\phi(x, \bar{r})e^{(ipx)}\,dx$$

$$\bar{r} = r\sqrt{1 - M_\infty^2} = r\beta$$

then the Fourier transformed solution of the perturbation potential from Eq. (1) is

$$\bar{\phi}(p, \bar{r}) = C_1 I_0(|p|\bar{r}) + C_2 K_0(|p|\bar{r}) \tag{2}$$

Received Sept. 22, 1993; revision received Dec. 25, 1993; accepted for publication Dec. 26, 1993.

*Graduate Student, Mechanical Engineering Department.
†Professor of Aerospace/Mechanical Engineering Department. Member AIAA.

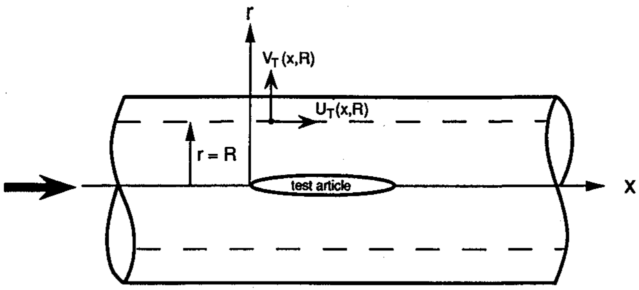

Fig. 1 Boundary value problem region of a wind-tunnel flowfield.

where I_0, K_0 are the zero order of the first and second kind of modified Bessel functions, respectively. $|p|$ is the absolute value of the Fourier transform parameter. C_1, C_2 are two constants to be determined from the boundary conditions.

By applying inverse Fourier transform to Eq. (2), the free-air velocity potential ϕ_∞ and the velocity potential generated by test article in a wind tunnel ϕ_T can be obtained with two different sets of boundary conditions, respectively. The difference between these two velocity potentials is called wind-tunnel wall interference ϕ_i. The test article body of revolution profile should be interpreted as a "potential equivalent" airfoil profile including the viscous effects. It is reasonable to assume that the same equivalent profile exists in a free-air flow condition. Two approaches in calculating blockage wall interference of the present two-variable method are based on two different model representations: 1) first approach—a profile of the body of revolution, and 2) second approach—a distribution of source-sink. They are described in the following text.

First Approach

Free-air flow solution. Assume the slope of a given body of revolution profile $S'(x)$, the boundary condition on the test article surface is

$$\lim_{\tilde{r}\to 0} \tilde{r}\frac{\partial\overline{\phi_\infty}(p,\tilde{r})}{\partial\tilde{r}} = \overline{S'}(p) \tag{3}$$

where

$$\overline{S'}(p) = \frac{1}{\sqrt{2\pi}}\int_{-\infty}^{+\infty} S'(x)e^{ipx}\,\mathrm{d}x$$

The far-field boundary condition for free-air flow in the Fourier transformed plane is

$$\lim_{\tilde{r}\to\infty} \overline{\phi_\infty}(p,\tilde{r}) = 0$$

Then, Eq. (2) becomes

$$\overline{\phi_\infty}(p,\tilde{r}) = -\overline{S'}(p)K_0(|p|\tilde{r}) \tag{4}$$

Tunnel flow solution. With the same body of revolution profile and a measured radial velocity distribution $V_T(x, R)$ or axial velocity distribution $U_T(x, R)$ on the tunnel test position $r = R$, the corresponding boundary conditions for tunnel flow potential $\overline{\phi_T}$ are

$$\frac{\partial\overline{\phi_T}(p,\tilde{R})}{\partial\tilde{r}} = \frac{1}{\beta}\overline{V_T}(p,\tilde{R})$$

or

$$\frac{\partial\overline{\phi_T}(p,\tilde{R})}{\partial x} = \overline{U_T}(p,\tilde{R})$$

$$\lim_{\tilde{r}\to 0} \tilde{r}\frac{\partial\overline{\phi_T}(p,\tilde{R})}{\partial\tilde{r}} = \overline{S'}(p)$$

where

$$\tilde{R} = R\beta$$

The tunnel flow potential $\overline{\phi_T}(p, \tilde{r})$ is then derived in terms of measured radial velocity $V_T(x, R)$ as

$$\overline{\phi_T}(p,\tilde{r}) = \left[\frac{\overline{V_T}(p,\tilde{R})}{\beta|p|I_1(|p|\tilde{R})} - \overline{S'}(p)\frac{K_1(|p|\tilde{R})}{I_1(|p|\tilde{R})}\right]I_0(|p|\tilde{r}) - \overline{S'}(p)K_0(|p|\tilde{r}) \tag{5a}$$

where I_1, K_1 are the first order of the first- and second-kind of modified Bessel functions, respectively. Similarly, the tunnel flow potential $\overline{\phi_T}(p, \tilde{r})$ can be determined in terms of measured axial velocity $U_T(x, R)$

$$\overline{\phi_T}(p,\tilde{r}) = \left[-\frac{\overline{U_T}(p,\tilde{R})}{ipI_0(|p|\tilde{R})} + \overline{S'}(p)\frac{K_0(|p|\tilde{R})}{I_0(|p|\tilde{R})}\right]I_0(|p|\tilde{r}) - \overline{S'}(p)K_0(|p|\tilde{r}) \tag{5b}$$

By combining Eqs. (5a) and (5b), the body of revolution profile function $\overline{S'}(p)$ is obtained as

$$\overline{S'}(p) = (\tilde{R}/\beta)\overline{V_T}(p,\tilde{R})I_0(|p|\tilde{R}) - (|p|/p)i\tilde{R}\overline{U_T}(p,\tilde{R})I_1(|p|\tilde{R}) \tag{6}$$

Therefore, $\overline{\phi_\infty}(p, \tilde{r})$ and $\overline{\phi_T}(p, \tilde{r})$ can be derived in terms of only the measured velocity components $\bar{U}_T(p, \tilde{R})$ and $\bar{V}_T(p, \tilde{R})$ at the control surface by substituting Eq. (6) into Eqs. (4) and (5a), respectively.

Interference flow solution. The wind-tunnel wall interference is defined as the difference between the wind tunnel and the free-air flow. Through the above derivation, the interference flowfield can be obtained directly related to the two measured tunnel flow variables U_T, V_T at the control surface, $r = R$, without explicitly in terms of body profile

$$\overline{\phi_i}(p,\tilde{r}) = \overline{\phi_T}(p,\tilde{r}) - \overline{\phi_\infty}(p,\tilde{r})$$

$$\overline{\phi_i}(p,r) = R\overline{V_T}(p,R)K_0(|p|\beta R)I_0(\beta r|p|) + i\beta R\frac{p}{|p|}\overline{U_T}(p,R)K_1(|p|\beta R)I_0(|p|\beta r) \tag{7}$$

with

$$\overline{U_T}(p,R) = \frac{1}{\sqrt{2\pi}}\int_{-\infty}^{+\infty} U_T(x,R)e^{ipx}\,\mathrm{d}x$$

$$\overline{V_T}(p,R) = \frac{1}{\sqrt{2\pi}}\int_{-\infty}^{+\infty} V_T(x,R)e^{ipx}\,\mathrm{d}x$$

Second Approach

The body of revolution profile is represented by a source-sink distribution. The velocity potential at any location inside the tunnel ϕ_T can be split into two parts: 1) tunnel wall interference potential ϕ_i and 2) the potential generated by test article in free-air ϕ_∞, $\phi_T = \phi_\infty + \phi_i$. The solution for the interference potential based on Eq. (1) is

$$\overline{\phi_i}(r,p) = B_1I_0(\beta r|p|) + B_2K_0(\beta r|p|) \tag{8}$$

Since K_0 is singular at $r = 0$, and $\overline{\phi_i}(r, p)$ is finite, the constant B_2 should be zero. Assuming $U_T(x, R)$ and $V_T(x, R)$ to be the measured axial and radial velocities at a specified tunnel test position $r = R$, the interference velocities $u_i(x, R)$ and $v_i(x, R)$ in Fourier transformed plane can be written as

$$\overline{u_i}(p, R) = \overline{\frac{\partial \phi_i(x, r)}{\partial x}}\bigg|_{r=R} = \overline{U_T}(p, R) + ip\overline{\phi_\infty}(p, R) \quad (9)$$

$$\overline{v_i}(p, R) = \overline{\frac{\partial \phi_i(x, r)}{\partial r}}\bigg|_{r=R} = \overline{V_T}(p, R) - \frac{\partial \overline{\phi_\infty}(p, r)}{\partial r}\bigg|_{r=R} \quad (10)$$

where

$$ip\overline{\phi_\infty}(p, R) = -\overline{\frac{\partial \phi_\infty(x, r)}{\partial x}}\bigg|_{r=R}$$

Combining Eqs. (8–10) to eliminate B_1 of Eq. (8), one obtains the following equation:

$$\frac{\overline{U_T}(p, R) + ip\overline{\phi_\infty}(p, R)}{-ipI_0(|p|\beta R)} |p| I_1(\beta R|p|) = \overline{V_T}(p, R) - \frac{\partial \overline{\phi_\infty}(p, r)}{\partial r}\bigg|_{r=R} \quad (11)$$

The free-air solution can be modeled by a distribution of source of strength $\sigma(x)$ per length along the body axis on the strip $0 \leq x \leq 1$. With this model, the perturbation velocity potential can be obtained by integrating the equations of the point source along the axis[5]

$$\phi_\infty(r, x) = -\frac{1}{4\pi}\int_0^1 \frac{\sigma(\xi)}{\sqrt{(x-\xi)^2 + \beta^2 r^2}} \, d\xi$$

By applying the Fourier transform and taking the coordinate transformation

$$x = \eta + \xi \quad \text{and} \quad \xi = \xi$$

the free-air potential in the Fourier transform plane can be derived[6] as

$$\overline{\phi_\infty}(r, p) = -\frac{1}{4\pi}\bar{\sigma}(p)\int_{-\infty}^{+\infty} \frac{e^{ip\eta}}{\sqrt{\eta^2 + \beta^2 r^2}} \, d\eta = -\frac{1}{2\pi}\bar{\sigma}(p)K_0(\beta r|p|) \quad (12)$$

where

$$\bar{\sigma}(p) = \frac{1}{\sqrt{2\pi}}\int_{-\infty}^{+\infty} \sigma(\xi)e^{ip\xi} \, d\xi$$

In order to solve the source strength distribution $\bar{\sigma}(p)$, the free-air potential $\overline{\phi_\infty}(p, R)$ given by Eq. (12) is substituted into Eq. (11)

$$\bar{\sigma}(p) = 2\pi R\left[\overline{V_T}(p, R)I_0(|p|\beta R) - i\frac{p}{|p|}\beta\overline{U_T}(p, R)I_1(|p|\beta R)\right] \quad (13)$$

By combining Eqs. (12) and (13) and the B_1 relation, Eq. (8) becomes

$$\overline{\phi_i}(r, p) = R\overline{V_T}(p, R)K_0(|p|\beta R)I_0(\beta r|p|) + i\beta R\frac{p}{|p|}\overline{U_T}(p, R)K_1(|p|\beta R)I_0(|p|\beta r) \quad (14)$$

The interference velocity potential of Eq. (14) is the same as Eq. (7) derived from first approach. With $\overline{u_i}(p, r) = -ip\overline{\phi_i}(p, r)$, the interference velocity in the transformed plan can be expressed as

$$\overline{u_i}(p, r) = -iR\overline{V_T}(p, R)pK_0(|p|\beta R)I_0(|p|\beta r) + \beta R\overline{U_T}(p, R)|p|K_1(|p|\beta R)I_0(|p|\beta r) \quad (15)$$

Solutions in the Physical Plane

The interference velocity in the physical plane can be obtained through inverse Fourier transformation from Eq. (15):

$$u_i(x, r) = \frac{1}{\sqrt{2\pi}}\int_{-\infty}^{+\infty} \overline{u_i}(p, r)e^{-ipx} \, dp = \frac{-iR}{2\pi}\int_{-\infty}^{+\infty} V_T(\eta, R)\left[\int_{-\infty}^{+\infty} pK_0(|p|\beta R) \times I_0(|p|\beta r)e^{ip(\eta - x)} \, dp\right] d\eta + \frac{\beta R}{2\pi}\int_{-\infty}^{+\infty} U_T(\eta, R)\left[\int_{-\infty}^{+\infty} |p|K_1(|p|\beta R) \times I_0(|p|\beta r)e^{ip(\eta - x)} \, dp\right] d\eta \quad (16)$$

The series expansion of Bessel functions has been used to integrate Eq. (16). For small r argument, I_0 can be expressed in a series form:

$$I_0(r) = 1 + (r^2/4) + \mathcal{O}(r^4)$$

By substituting the series expansion of I_0 into Eq. (16), the final form of the axial interference velocity $u_i(x, r)$ can be obtained through a sequence of manipulation

$$u_i(x, r) = \frac{R}{2}\int_{-\infty}^{+\infty} V_T(\eta, R)\frac{(\eta - x)}{[(\eta - x)^2 + \beta^2 R^2]^{3/2}} \, d\eta + \frac{9r^2}{8\beta^3 R^4}\int_{-\infty}^{+\infty} V_T(\eta, R)(\eta - x) \times F\left[\frac{5}{2}, \frac{5}{2}, \frac{3}{2}, -\frac{(\eta - x)^2}{\beta^2 R^2}\right] d\eta + \frac{\beta^2 R^2}{2}\int_{-\infty}^{+\infty} \frac{U_T(\eta, R)}{[(\eta - x)^2 + \beta^2 R^2]^{3/2}} \, d\eta + \frac{3r^2}{8\beta R^3}\int_{-\infty}^{+\infty} U_T(\eta, R)F\left[\frac{5}{2}, \frac{3}{2}, \frac{1}{2}, -\frac{(\eta - x)^2}{\beta^2 R^2}\right] d\eta \quad (17)$$

where F is a hypergeometric function.[6] The interference pressure coefficient can then be obtained as $C_{p_i} = -2u_i$. Equation (17) indicates that the interference velocity component is expressed in terms of only two measured variables $U_T(x, R)$ and $V_T(x, R)$ at the control surface.

Numerical Examples

Open Jet Tunnel

To validate the above derived formula, a numerical example was performed by the modified TSFOIL code[3,7] for a given model geometry

$$r/l = 4\varepsilon x(1.0 - x)$$

in an open jet tunnel, where ε is the ratio of the maximum body thickness r_{max} to l. The selected case has the model to

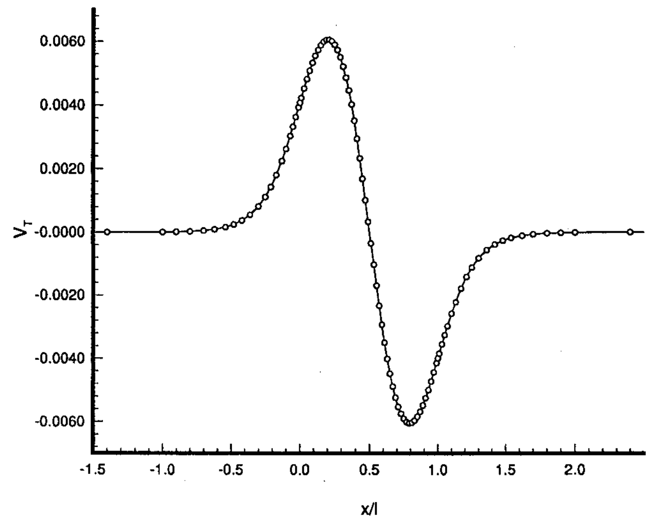

Fig. 2 Radial velocity distribution calculation from TSFOIL at the interface R/l = 0.82.

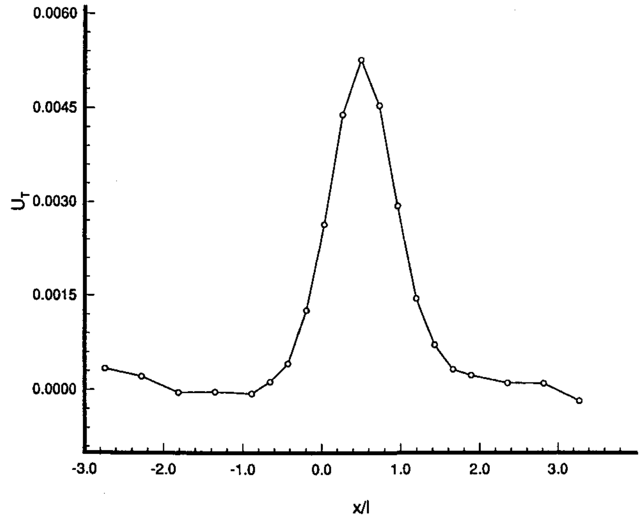

Fig. 4 Axial velocity distribution calculated from PMARC code at the interface R/l = 0.82.

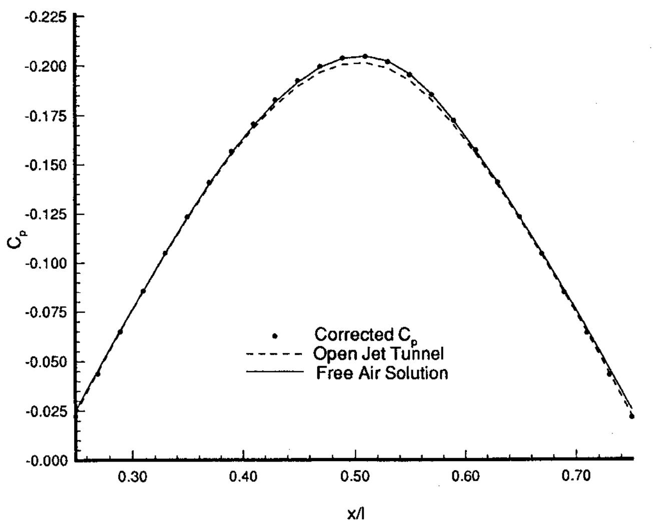

Fig. 3 Pressure coefficient correction on the model of the body of revolution in an open jet wind tunnel, at M_∞ = 0.9.

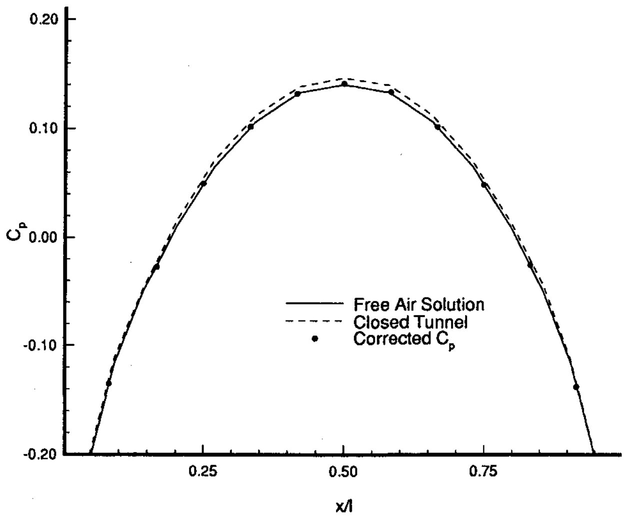

Fig. 5 Pressure coefficient correction in a closed tunnel.

tunnel blockage ratio 1%, Mach number M_∞ = 0.9, and the ratio of the tunnel radius to the length of the test article R/l = 0.82. For an open jet tunnel, the axial velocity on the tunnel wall is zero, i.e., $U_T(x, R) = 0$. By selecting the control surface at the tunnel wall, the radial velocity distribution $V_T(x, R)$ calculated from the TSFOIL code as shown in Fig. 2 is substituted into Eq. (17) as the required variable to determine the interference velocity and pressure coefficient at the model plane. By subtracting the C_{p_i} from the open jet pressure coefficient of TSFOIL data, the free-air pressure coefficient C_{p_∞} is obtained. Figure 3 shows the comparison of the corrected C_{p_∞} distribution with the reference data. It is seen that the tunnel data with the correction from Eq. (17) gives good agreement with free-air flow results.

Closed Tunnel

The second numerical example obtained from the PMARC code[4] is a closed tunnel case. A test article with the same parabolic body of revolution geometry as shown in an open-jet tunnel is tested in a closed circular tunnel. The flow is incompressible, and the ratio of the tunnel radius to the length of the length of the test article is 0.82. The blockage ratio is 1%. For the closed wind tunnel, the radial velocity $V_T(x, R)$ at the tunnel wall is zero. In order to obtain the other required variable for the derived formula Eq. (17), a panel method code PMARC was used to calculate the axial velocity profile $U_T(x, R)$ on the closed wind-tunnel wall, as shown in Fig. 4. The interference velocity and pressure coefficient was calculated by substituting $U_T(x, R)$ into Eq. (17). Figure 5 shows the comparison of the interference pressure coefficients between solution of the two-variable method and PMARC code. Good agreement can be seen in Fig. 5. These results have clearly demonstrated that the two-variable method for circular tunnel blockage wall interference assessment is promising for experimental verification.

Concluding Remarks

Analytical expressions are obtained for the blockage wall interference in a circular tunnel as a function of two measured velocity components at the control surface or the tunnel wall. The solutions are derived by assuming two types of representation of the body of revolution as testing article. The analytic solutions are verified by numerical examples computed by two inviscid codes for open jet and closed tunnels.

Acknowledgments

This work was partially supported by NASA Ames Research Center under Grant NAG 2-733 with technical monitor F. W. Steinle Jr.

References

[1]Mokry, M., and Erickson, J. C., Jr., "Fluid Dynamics Panel Working Group 12 on Adaptive Wind Tunnel Walls: Technology and Applications," AGARD-AR-269, April 1990, pp. 66–90.

[2]Lo, C. F., "Tunnel Interference Assessment from Measurements on Two Interfaces," *AIAA Journal*, Vol. 28, No. 8, 1990, pp. 1481–1484.

[3]Lo, C. F., and Sickles, W. L., "Analytic and Numerical Investigation of the Convergence for the Adaptive Wall Concept," Arnold Engineering Development Center, AEDC-TR-79-55, Arnold Air Force Base, TN, Nov. 1979.

[4]Ashby, D. L., Dudley, M. R., Iguchi, S. K., Browne, L., and Katz, J., "Potential Flow Theory and Operational Guide for the Panel Code PMARC," NASA TM-102851, Jan. 1991.

[5]Katz, J., and Plotkin, A., "Low-Speed Aerodynamics: From Wing Theory to Panel Methods," McGraw-Hill, New York, 1991, pp. 227, 228.

[6]Gradshteyn, I. S., and Ryzhik, I. M., "Table of Integrals, Series, and Products," Academic Press, New York, 1980, pp. 747, 749, 961.

[7]Murman, E. M., Bailey, F. R., and Johnson, M. L., "TSFOIL—A Computer Code for Two-Dimensional Transonic Calculations, Including Wind-Tunnel Wall Effects and Wave-Drag Evaluation," NASA SP-347, March 1975, pp. 769–788.